Nat Hazards
DOI 10.1007/s11069-006-9026-9

ORIGINAL PAPER

A GIS-based methodology for hazard mapping of small volume pyroclastic density currents

G. P. Toyos · P. D. Cole · A. Felpeto · J. Martí

Received: 19 September 2005 / Accepted: 22 May 2006

Abstract We present here a methodology implemented within a geographical information system (GIS) for hazard mapping of small volume pyroclastic density currents (PDCs). This technique is implemented as a set of macros written in Visual Basic for Applications (VBA) that run within GIS-software (i.e. ArcGIS). Based on the energy line concept, we calibrated an equation that relates the volume (V) and the mobility ($\Delta H/L$) of single PDCs using data from Soufrière Hills volcano (Montserrat) and Arenal volcano (Costa Rica). Maximum potential run-outs can be predicted with an associated uncertainty of about 30%. Also based on the energy line concept and with data from Soufrière Hills volcano and Mt. St. Helens (USA), we were able to calibrate an equation that predicts the flow velocity as a function of the vertical distance between the energy line and the ground surface (Δh). Velocities derived in this way have an associated uncertainty of 3 m s^{-1}. We wrote code to implement these equations and allow the automatic mapping of run-out and velocity with the inputs being (i) the height and location of the vent (ii) the flow volume and (iii) a digital elevation model (DEM) of the volcano. Dynamic pressure can also be estimated and mapped by incorporating the density of the pyroclastic density current (PDC). This computer application allows the incorporation of uncertainties in the location of the vent and of statistical uncertainties expressed by the 95% confidence limits of the regression model. We were able to verify predictions by the proposed

G. P. Toyos (✉) · P. D. Cole
Department of Geography, Environment and Disaster Management, Coventry University, Priory St., Coventry CV1 5FB, UK
e-mail: wtoyos@hotmail.com

A. Felpeto · J. Martí
Institute of Earth Sciences ''Jaume Almera'', CSIC, Lluis Sole Sabaris s/n, 08028 Barcelona, Spain

Present Address:
G. P. Toyos
Comisión Nacional de Actividades Espaciales (CONAE)
Av. Paseo Colón 751, 1063 - Buenos Aires
Argentina

methodology with data from Unzen volcano (Japan) and Mayon volcano (The Philippines). The consistencies observed highlight the applicability of this approach for hazard mitigation and real-time emergency management.

Keywords Pyroclastic density current · Hazard mapping · GIS · Run-out · Velocity · Dynamic pressure · Volume · Energy line · Mobility

1 Introduction

Volcanic hazard assessment has traditionally entailed geological mapping of volcanic deposits, the application of empirical approaches or of complex physical models (e.g. Esposti Ongaro et al. 2002; Todesco et al. 2002; Saucedo et al. 2005; Sheridan et al. 2004). Although sophisticated models may more accurately represent the true complexity of volcanic phenomena, simple empirical approaches, often requiring a limited number of parameters, can be useful decision-support tools for real-time hazard mitigation, such as during volcanic crises when decision-making needs to be fast (Malin and Sheridan 1982).

This paper presents a methodology for hazard mapping of small volume, gravity-driven PDCs. On the basis of the energy line concept (Hsü 1975; Malin and Sheridan 1982) (Fig. 1) and statistical analysis we have developed a set of tools for the prediction and mapping of flow maximum potential run-out, maximum potential velocity and dynamic pressure. We used data from PDCs at Soufrière Hills volcano, Montserrat (West Indies), Arenal volcano (Costa Rica) and Mt. St. Helens (USA). At Montserrat, gravitationally-driven PDCs with run-outs of 1–7 km were formed by partial collapses of an andesitic lava dome between 1996 and 1997 and also by fountain collapse associated with vulcanian explosions in 1997 (Calder et al. 1999; Calder et al. 2002; Cole et al. 2002 and Loughlin et al. 2002). Basaltic-andesitic PDCs with run-outs of 1–4 km formed at Arenal volcano by partial collapse of the crater region between 1992 and 2001 (Alvarado and Soto 2002; Cole et al. 2005). At Mt. St. Helens, the PDCs were formed by fountain collapse associated with explosions in August 1980 (Hoblitt 1986; Levine and Kiefer 1991). Thus, the methodology is based on dome forming volcanoes and small stratocones and is therefore equally applicable to either.

We have calculated empirical formulae, which are implemented as portable GIS-macros, written in Visual Basic for Applications (VBA) and running within ArcGIS, to enable the automatic production of hazard maps. One of the main challenges of

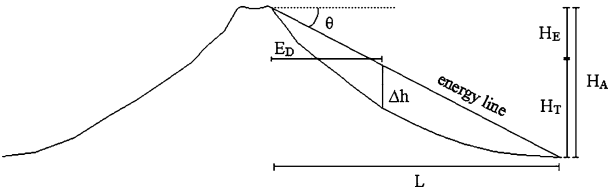

Fig. 1 Diagram explaining the energy line concept. The mobility ratio ($\Delta H/L$) is defined by the drop in height (H_A) over the run-out distance (L) and the energy line forms a depression angle (θ) with the horizontal. The parameters used by the algorithm to derive the maximum run-out of PDCs within ArcGIS are also indicated, i.e. E_D = Euclidean distance from the source centre, $H_E = E_D \times \Delta H/L$ ($\Delta H = H_A$), H_A = DEM-elevation + user-defined altitude above the source centre, H_T (energy cone elevation) $= H_A - H_E$, $\Delta h = H_T$ – DEM-elevation

volcanic hazard mapping is caused by the uncertainties related to the process itself, the data, the parameterisation of models and their subsequent sensitivity (Renschler 2005). In these respects, this study investigates the residuals of the regression models; the code allows the automatic delineation of the maximum confidence limits of the regression model and multiple source simulations are possible for the run-out of PDCs. We preferred GIS-embedded computer programming to loosely-coupled modelling (Burrough and McDonnel 1999), where the main algorithm performs the calculations outside the GIS, since programming within the GIS environment enables the development of graphic-user interfaces (GUIs) without losing the functionality of the GIS-software (e.g. ArcGIS). Finally, we verify the proposed methods with data from Unzen volcano (Japan) (Nakada et al. 1999) and Mayon volcano (The Philippines) (Moore and Melson 1969).

2 Statistical analysis

The energy line concept constitutes the basis for the methodology presented by this paper, both for the prediction of the run-out and the velocity of PDCs. The energy line concept was originally conceived for rock avalanches (Hsü 1975) and has been further extended to several gravity-driven phenomena, such as PDCs (Malin and Sheridan 1982; Hayashi and Self 1992) and debris avalanches (Siebert 1984). It uses the 'energy line' that links the location of the source of the phenomenon with the distal limit of the flow deposit (Fig. 1). The tangent of the angle of this line relative to the horizontal represents the resistance due to friction (Malin and Sheridan 1982; Sheridan and Malin 1983) and is characterised by the ratio between the vertical descent (ΔH) over the distance run-out (L) and is also known as the Heim coefficient or mobility ratio ($\Delta H/L$). This has been commonly used to illustrate the mobility of a variety of flow phenomena including debris avalanches (Siebert 1984), PDCs (Hayashi and Self 1992) and debris flows (Iverson 1997).

2.1 Maximum potential run-out

The energy line was extended 360° around volcanoes by Malin and Sheridan (1982) to define an energy cone. The intersection between this cone and topography defines the maximum potential run-out of PDCs (Fig. 1).

We undertook regression analysis to relate the volume and the mobility ratio of both dome-collapse or crater-wall-collapse and fountain-collapse types of PDCs occurred at Soufrière Hills volcano, Montserrat during 1996 and 1997 (Calder et al. 1999; Calder et al. 2002; Cole et al. 2002) and at Arenal volcano (Costa Rica) in 1993, 1998, 2000 and 2001 (Alvarado and Soto 2002; Cole et al. 2005) (Table 1). Typically, dome-collapse events involve numerous PDCs (Cole et al. 2002; Alvarado and Soto 2002). As a consequence, estimating the mobility using the total volume of PDCs produced by a dome-collapse or crater-wall collapse event is likely to result in significant underestimates. Relationships produced by previous workers, such as Hayashi and Self (1992) and Calder et al. (1999) will include such an underestimation. This might also partly explain the apparent higher mobility of single pulse fountain-collapse derived PDCs when compared to dome-collapse events (Calder et al. 1999). In this study, we have considered volumes associated with only one single PDC. We considered those events that were known to be generated by a single

Table 1 Date, type, volume, number of pulses, averaged volume, vertical descent (ΔH), distance run-out (L), mobility ratio ($\Delta H/L$) and depression angle (θ) of PDCs occurred at Soufrière Hills volcano, Montserrat (West Indies) (Calder et al. 1999; Cole et al. 2002) and Arenal volcano (Costa Rica) (Alvarado and Soto 2002; Cole et al. 2005)

Date	Location	Type	Volume (m^3)	# pulses	Volume_av (m^3)	ΔH (km)	L (km)	$\Delta H/L$	θ (°)
03-04-96	M (TR)	DC	1.5×10^5	3	5.1×10^4	0.6	1.2	0.50	27
12-05-96	M (TR)	DC	3.3×10^5	3	1.1×10^5	0.9	2.4	0.38	21
30-03-97	M (WR)	DC	2.6×10^6	6	4.3×10^5	0.8	2.6	0.31	17
11-04-97	M (WR)	DC	2.9×10^6	6	4.8×10^5	0.9	3.1	0.29	16
05-06-97	M (Tuitts)	DC	3.8×10^5	1	3.8×10^5	0.9	2.6	0.35	19
17-06-97	M (Mos)	DC	7.7×10^5	4	1.9×10^5	0.9	3.0	0.30	17
25-06-97$_a$	M (Mos)	DC	7.8×10^5	1	7.8×10^5	1.0	3.5	0.28	16
25-06-97$_b$	M (Mos)	DC	2.4×10^6	1	2.4×10^6	1	4.7	0.21	12
25-06-97$_c$	M (Mos)	DC	2.4×10^6	1	2.4×10^6	1	4.7	0.21	12
03-08-97	M (FG)	DC	8.8×10^6	6	1.5×10^6	0.9	5.1	0.18	10
21-09-97	M (Tuitts)	DC	1.4×10^7	2	6.8×10^6	0.9	5.5	0.17	10
18-10-97	M (FG)	FC	1.4×10^5	1	1.4×10^5	1.2	4.7	0.26	14
19-10-97	M (WR)	FC	8.2×10^4	1	8.2×10^4	1.3	4.1	0.31	17
20-10-97	M (Tuitts)	FC	2.0×10^4	1	2.0×10^4	1.1	2.9	0.37	21
21-10-97	M (TR)	FC	6.3×10^4	1	6.3×10^4	1.1	3.0	0.37	20
1993	Arenal	CWC	2.2×10^6	4	5.5×10^5	–	3.2	0.34	19
1998	Arenal	CWC	5.0×10^5	23	2.2×10^4	–	2.0	0.46	25
2000	Arenal	CWC	2.0×10^6	27	7.4×10^4	–	2.3	0.40	22
2001	Arenal	CWC	2.4×10^5	24	1.0×10^4	–	2.0	0.46	25

Location refers to the streams: M = Montserrat, TR = Tar river, WR = White river, Mos = Mosquito Ghaut, FG = Fort Ghaut; DC: dome-collapse PDCs; FC: fountain-collapse PDCs (pumice flows); CWC: crater wall collapse; Volume_av: Volume/# pulses

PDC, where volumes for several individual PDCs were known, or we used data from events where the number of individual PDCs within a dome-collapse event was relatively well known and averaged the total volume of the collapse event with the number of individual flows or pulses (Table 1).

This analysis resulted in a significant regression model ($P < 0.01$) and a good statistical fit ($r^2 = 0.77$) (Fig. 2) for the relationship between PDC volume (V) and mobility ($\Delta H/L$):

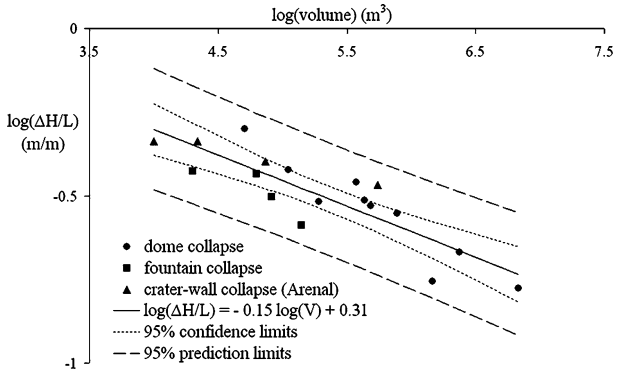

Fig. 2 Log–normal relationship between the volume and the mobility index of dome- and fountain-collapse PDCs from Soufrière Hills volcano, Montserrat, and of PDCs originated from crater-wall collapse at Arenal volcano (Costa Rica) combined with the line predicted by the equation and the 95% confidence and prediction limits

$$\Delta H/L = 2.03V^{-0.15} \quad (1)$$

Thus, for a given PDC volume, this relationship (Eq. 1; Fig. 2) allows the prediction of the mobility ratio ($\Delta H/L$) and in turn of the run-out, provided knowledge on the location and elevation above sea level of the source centre is available. In order to obtain an idea of the precision of this equation, we simulated (see section 3.1) all the flows considered in the calibration (Table 1) and computed the average misfit (%) and the root mean square error (RMSE), as shown by Eqs. 2, 3, respectively:

$$\text{Average misfit (\%)} = \sum[(p-a)_i 100a^{-1}]/n \quad (2)$$

$$RMSE = \sum[(p-a)^2/n]^{1/2} \quad (3)$$

where p is the run-out that corresponds to the mobility ratio ($\Delta H/L$) predicted at the regression line, a is the actual run-out and n is the number of observations. We obtained an average misfit of 27% and a RMSE of 0.8 km. These results suggest an horizontal length for hazard zones based on this methodology not smaller than 0.8 km. The confidence limits of the regression model (Fig. 2) may also be used as additional safety margins.

2.2 Maximum potential velocity

The maximum potential velocity of PDCs can also be derived on the basis of the energy line concept by assuming a complete conversion of potential into kinetic energy:

$$v = [2g\Delta h]^{1/2} \quad (4)$$

where v is the velocity, g is the acceleration due to gravity (9.81 m s^{-2}) and Δh is the vertical distance between the energy line and the ground surface (Fig. 1). We used data on velocities of the 25 June 1997 PDCs at Soufrière Hills volcano (Loughlin et al. 2002) and of the 7 August 1980 event at Mt. St. Helens (Levine and Kiefer 1991) (Table 2) to calibrate the general form of the relationship between v and Δh (Fig. 1):

$$v = a\Delta h^b \quad (5)$$

where Δh is constrained by the mobility ratio, and $a = (2g)^{1/2}$ and $b = 1/2$ if only the resistance due to friction is considered. We undertook regression analysis with the linear form of Eq. 5 and obtained a good fit ($r^2 = 0.76$) (Fig. 3) between the observed velocities and the vertical distance between the energy line and the surface (Δh) (Table 2) and obtained the relationship:

$$v = 0.38\Delta h^{0.68} \quad (6)$$

Other workers have parameterised the flow's shear resistance to account for the effects of viscosity and turbulence (e.g. McEwen and Malin 1989; Sheridan and Macías 1992; Kover 1995; Sheridan et al. 2000). However, here we used the coefficients a and b (Eq. 5) to account for all the factors that force the flow to stop.

As with the run-out regression model, we computed the average misfit (%) and the RMSE (see section 2.1). In this case, p and a (Eqs. 2, 3) correspond to the

Table 2 Summary of data used in the statistical calibration (Loughlin et al. 2002; Levine and Kiefer 1991). The values of Δh were constrained with the energy line of each current considered and estimated at the cells that correspond to each velocity measurement

Soufrière Hills		Mt. St. Helens	
Δh (m)	Velocity (m s^{-1})	Δh (m)	Velocity (m s^{-1})
52	8.0	75	7
86	10.0	113	7
143	11.0	153	9
183	15.0	193	10
250	16.1	273	17
215	16.7	313	17
236	20.0	361	17
287	20.2	382	17
264	21.9	312	20
		380	22
		342	22
		370	25
		324	27
		385	30

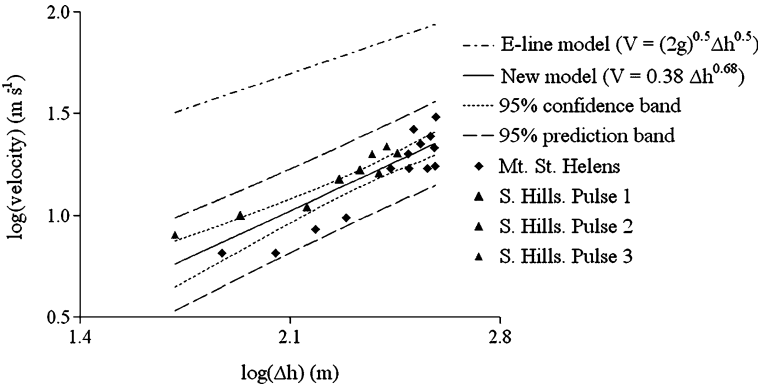

Fig. 3 Empirical relationship between the vertical distance between the energy line and the surface(Δh) and the flow velocity (New model), 95% confidence and prediction limits, and both the observed and e-line velocities corresponding to the same Δh, where measurements were carried out

velocity predicted by Eq. 6 and the actual value (Table 2), respectively. We obtained an average misfit of ~18% and a RMSE of ~3m s^{-1}. The velocities predicted by this procedure are between 4 and 6 times smaller than those that would be predicted by the original equation that considers only the resistance due to friction. These ranges of uncertainty are useful to define the scale of hazard maps and for the calibration of numerical models and of approaches that enable the quantification of the physical damage and casualties.

3 GIS-implementation

We developed a computer application that implements Eqs. 1 and 6 to allow the automatic production of maps of maximum run-out, velocity and dynamic pressure of PDCs. Code was written in VBA and deployed as a template file from which any ArcGIS project can be derived. The inputs for this procedure can be provided via GUIs that use non-technical terms (Fig. 4), hence allowing non-expert use.

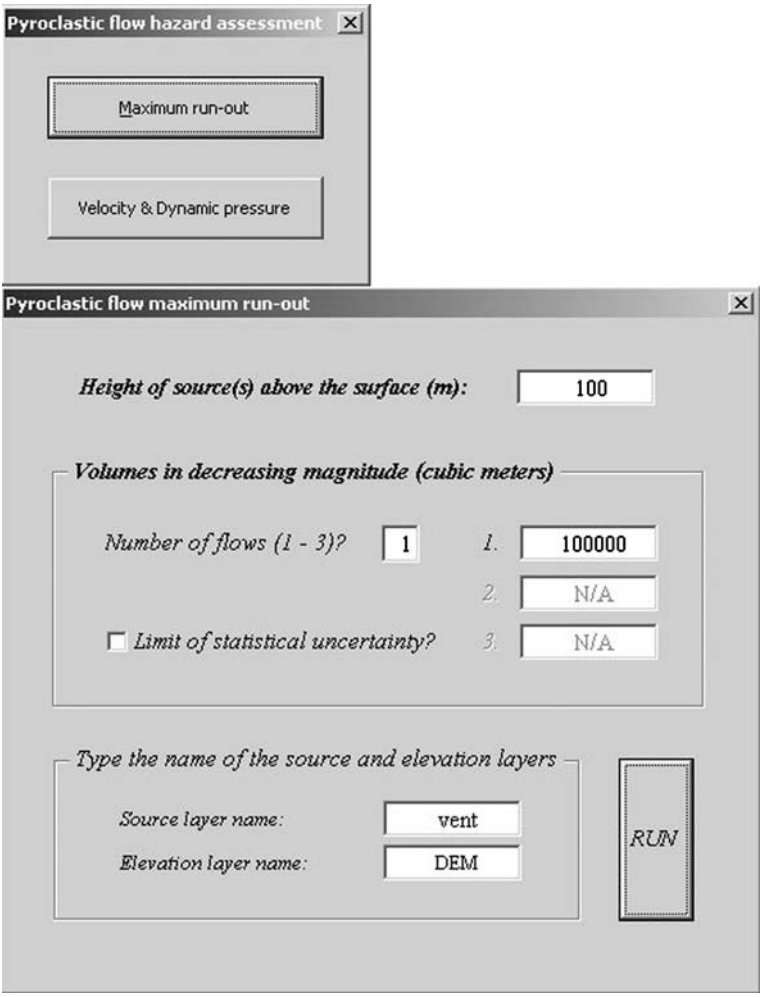

Fig. 4 Graphic-user interface for the inputs to simulate PDC maximum potential run-out

3.1 Run-out

We used the prediction of maximum potential run-out as the first step towards the definition of hazard zones. Fig. 5 summarises the methodology used for this technique.

The computer application implements Eq. 1 and uses as input: a vector point layer that represents the source and a raster layer with elevation data (DEM). The user specifies (i) the height of the source above the surface (ii) up to three PDC volumes and (iii) the names of the vector and DEM layers (Fig. 4). For each of the user-selected volumes the code uses equation 1 to calculate the $\Delta H/L$ and uses the algorithm (Fig. 5) to find the intersection of the energy line with topography, which defines the maximum extent of the PDC. The program assigns the cells within the energy cone a value of 1 and the cells outside the energy cone a value of 0. The

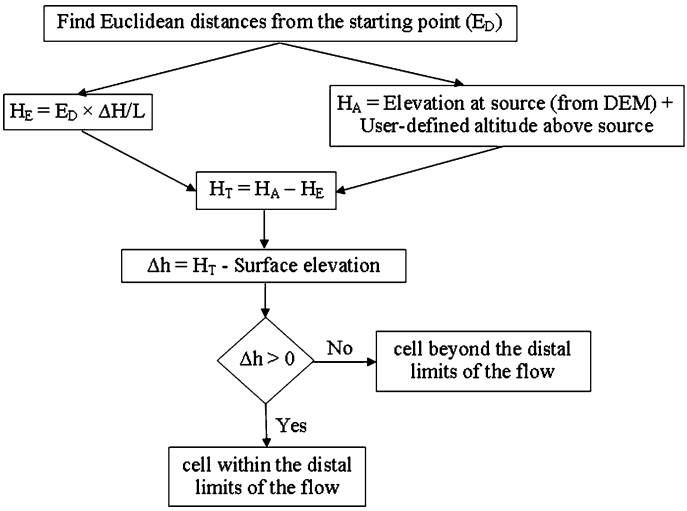

Fig. 5 Flow diagram describing the principal algorithm used to define the energy cone. If the cell is within the distal limits of the current, then the cell has a value of 1, otherwise it has a value of 0. For the graphic representation of the parameters please refer to Fig. 1

graphic output is a vector layer with a line that delineates the maximum limit that would be reached by the flow around the volcano (Fig. 6).

The delineation of the maximum extent of PDCs by this procedure (Fig. 5) is realistic only in the absence of natural barriers (e.g. Alberico et al. 2002). If a topographic barrier that intersects the energy line exists (Fig. 7), then the original algorithm (Fig. 5) will consider some of the cells located further downstream of such barrier to be within the limits defined by the intersection of the energy cone with topography (Fig. 7). Thus, these cells will have value of 1 when the flow under consideration would never reach them in reality. To make output maps more realistic, the computer programme includes a routine that performs a correction assigning a value of zero to the cells located beyond topographic barriers, which would be erroneously considered to be located within the limits defined by the energy cone (Fig. 7).

The option 'Limit of uncertainty' (Fig. 4) allows the user to delineate the upper 95% confidence limit of the regression model. We adopted a conservative approach and, therefore, we made the code able to delineate only the upper and not both the upper and lower limits of statistical uncertainty. Since this is a t-test of two tails (Draper and Smith 1966) the upper 95% confidence limit indicates that there is actually 97.5% chance that the PDC will remain within this boundary. The program generates two layers, one for the maximum extent and the other one for the upper confidence limit (Fig. 6). This limit accounts for the statistical uncertainty around the mean value of the mobility predicted by the regression model.

Multiple source runs are also possible and are performed automatically if the input vector layer has more than one source centre. The program loops as many times as the number of potential 'vents', adds the grids cumulatively (cell values are 1 or 0 depending on whether they are within or outside the energy cone) and finally divides the value of each cell by the number of sources and multiplies it by 100. Thus, the user obtains as output a grid of percent probability ranging between 0 and 100%.

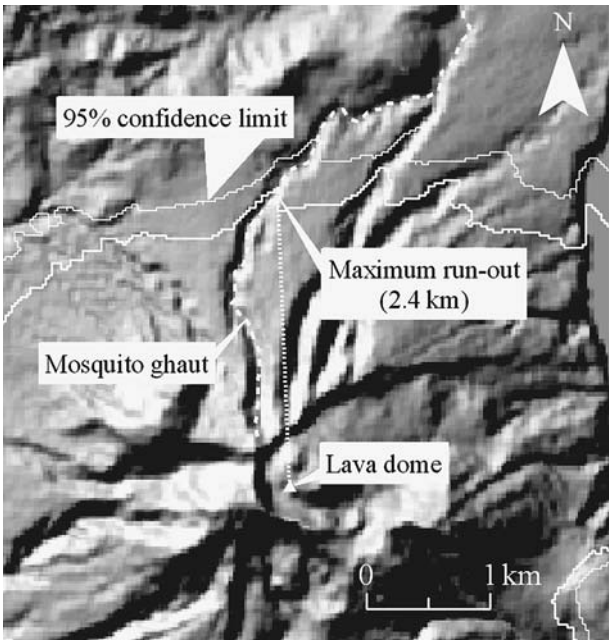

Fig. 6 Sample output of a dome-collapse PDC that occurred on 17 June 1997 at Soufriére Hills volcano, Montserrat (West Indies) and flowed down Mosquito Ghaut reaching 3.0 km from the source(Table 1). The flow volume was ~1.9×10^5 m^3 and we assumed the height of the lava dome to be of 300 m above the topography available (Calder et al. 1999; Cole et al. 2002). We used a 25-m cell DEM derived from digital contours of scale 1:25000

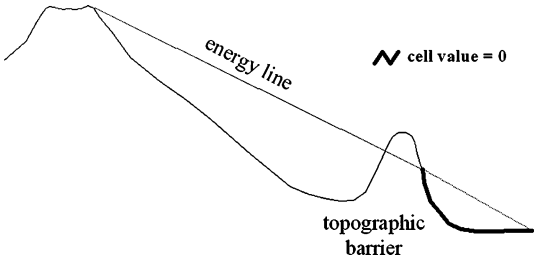

Fig. 7 Diagram describing the basis for the correction for natural barriers. The bold line indicates the cells, which the original algorithm (see Fig. 5) would consider erroneously to be within the energy cone. The routine performs the correction by assigning these cells a value of zero

Above this layer a vector layer is also generated, which delineates the maximum extent of all flows together. This routine allows a first order approximation to the incorporation of the uncertainty in the location of potential vents into hazard maps, assuming that the probability of an eruption through any of the vents is the same. This uncertainty can be critical in the context of large caldera volcanoes such as Sete Cidades in the island of São Miguel, Azores (Portugal) (Fig. 8), Teide in the island of Tenerife, Canaries (Spain), Campi Flegrei (Italy), etc.

3.2 Velocity and dynamic pressure

The potential velocity and the dynamic pressure of PDCs are critical parameters as regards the impact of these phenomena on infrastructure (e.g. Valentine 1998;

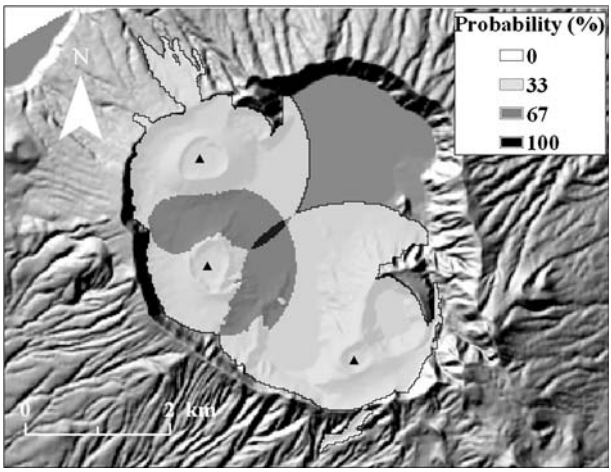

Fig. 8 Sample output of a scenario for PDCs of 1×10^6 m^3 and a height of 250 m above 3 potential sources at Sete Cidades volcano in the island of São Miguel, Azores (Portugal). The legend indicates the probability of the current reaching the corresponding cells. This figure is for illustrative purposes, since it does not represent any real event. We used a DEM of 25 m cell size derived from digital contours of 1:25000 scale

Spence et al. 2004). The implementation of the equation to derive the flow velocity within ArcGIS is possible by using the value of Δh to estimate the velocity at each cell of the output grid, in contrast to using Δh as a decision rule for the derivation of the energy cone (Figs. 1, 5). To enable the generation of velocity maps we implemented Eq. 6 (Fig. 3). This application allows also the generation of maps of dynamic pressure (P_{dy}), which is estimated by incorporating the flow density (ρ) as follows (e.g. Valentine 1998; Spence et al. 2004):

$$P_{\mathrm{dy}} = 0.5\rho v^2 \tag{7}$$

The user-specified inputs are (i) the height at the source above the surface (ii) the volume of the PDC or the depression angle (Fig. 1), which enables the production of maximum potential run-out and velocity/pressure maps of the same event and (iii) the names of the vector and DEM layers (Fig. 9). The 'Advanced' option allows users to set their own coefficients (i.e. a and b of Eq. 5 (if available)). To obtain dynamic pressure users must input the density of the flow in kg m^{-3} (Fig. 9). The output of this application is either a velocity (m s^{-1}) and/or a dynamic pressure (kPa) grid and overlain onto this grid is a vector layer that defines the maximum potential extent of the flow (Fig. 10).

4 Discussion

We have developed a set of tools that allows the automatic production of hazard maps on the basis of maximum potential run-out, maximum potential velocity and dynamic pressure of small volume PDCs. In order to have an idea of the accuracy of this approach, we used PDC events that occurred in Unzen (Japan) and Mayon (The

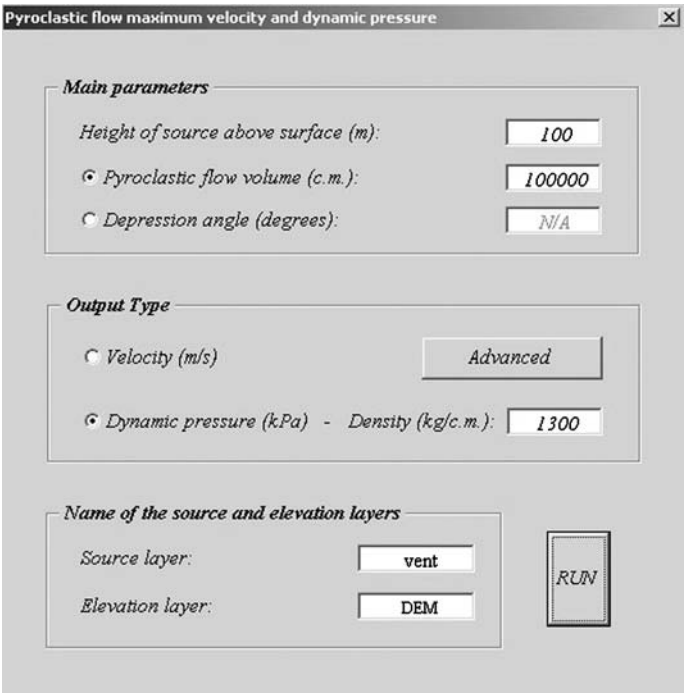

Fig. 9 Graphic-user interface for the inputs of velocity and/or dynamic pressure runs

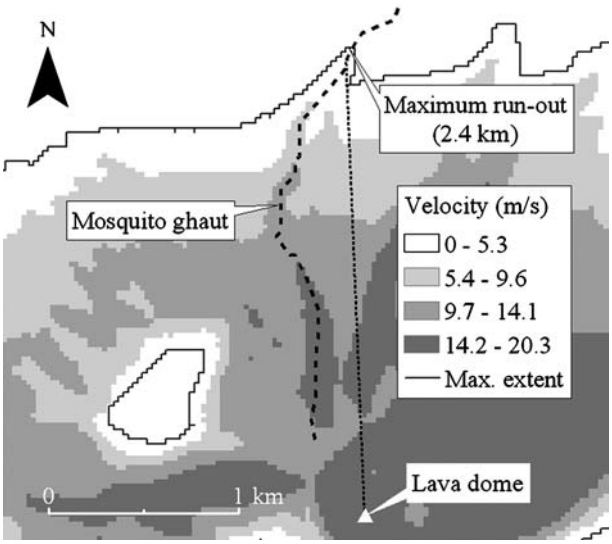

Fig. 10 Sample output of the velocity (m s^{-1}) of the PDC of 17 June 1997 that travelled 3.0 km down Mosquito Ghaut at Soufriére Hills volcano, Montserrat (West Indies). The inputs, assumptions and digital topography employed are the same as those used for the run shown by Fig. 6

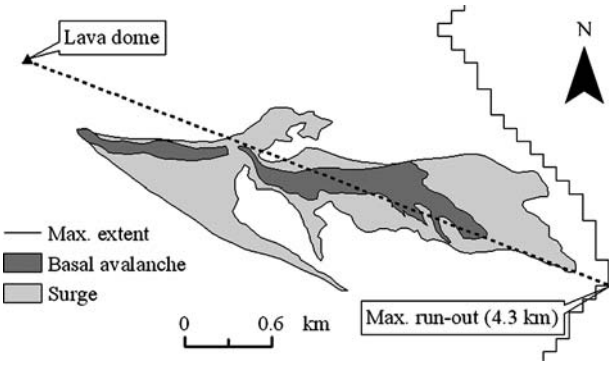

Fig. 11 Verification at Unzen volcano (Japan): the figure shows the deposits of the dome-collapse PDC of 3 June 1991 of 5.0×10^5 m^3 that reached ~4 km from the source (Nakada et al. 1999). The methodology predicts a run-out of 4.3 km. The legend discriminates between basal avalanche and surge deposits. The lava dome was located at 1,280 m on the eastern slope of Mt. Unzen

Philippines) volcanoes and tested the run-outs and velocities that can be predicted by this methodology.

On 3 June 1991, a block-and-ash flow of $5.0 \times 10^5 m^3$ descended the slopes of Mt. Unzen (Japan) reaching about 4 km from the source (Fig. 11). On 15 September 1991, the last flow ($1.0 \times 10^6 m^3$) of a series of dome-collapse events reached approximately 5.5 km from the emission centre (Nakada et al. 1999). Assuming the source of the PDC to be located at an altitude of 1,280 m on the eastern slope of the Mt. Unzen and using a DEM of 90 m cell size available from the internet, i.e. data from the Shuttle Radar Topographic Mission (SRTM) of the United States Geological Survey (USGS) (http://www.srtm.usgs.gov/), the methodology proposed was able to predict run-outs of 4.3 and 4.8 km for the former and the latter events, respectively. Thus, model predictions are within 300 and 700 m from the actual values in the first and second case, respectively (Fig. 11).

These results suggest acceptable levels of accuracy for the approach proposed. However, the volume of each event corresponds to an individual PDC or pulse within a multiple event dome collapse. Thus, averaging the volume by the number of pulses was not necessary, a fact that reduced the probability of overestimating the run-out. Besides, the good matches reflect that the volume calculations were well constrained. In other words, the statistical calibration is highly sensitive to the quality of the volume calculations and especially to the number of pulses. This is not surprising since the estimation of both involves high levels of uncertainty. The dataset we used in the statistical calibration (Table 1) contains only well-constrained volume data, hence the good statistical fit obtained.

As regards the velocity, we were able to carry out a comparison of a run that aimed at reproducing the velocities of a PDC that occurred on 2 May 1968 in Mayon volcano (The Philippines) with velocity measurements based on movies (Moore and Melson 1969). We used the vertical descent and the distance run-out of this event to constrain its depression angle, a fountain-collapse height of 500 m above the summit of the volcano (Moore and Melson 1969) and a 90 m cell size DEM from the internet (SRTM data). For the same 2-km path, the velocities obtained are consistent with those reported in the literature (Moore and Melson 1969). Moore and Melson (1969)

reported an average velocity of 31 m s^{-1}, while we obtained an average value of 27 m s^{-1} on the basis of a sample of 14 points along the PDC path.

In summary, the set of tools presented herein predicts run-outs and velocities that are consistent with measurements reported elsewhere (Nakada et al. 1999; Moore and Melson 1969). This provides preliminary quantitative support for the application of this methodology for hazard mapping of small volume PDCs at other volcanoes.

5 Conclusions

Hazard mapping of small volume PDCs triggered by gravitational collapse of domes, crater-wall- or by fountain-collapse is possible by using simple approaches that require as input a limited number of parameters and modest computer resources.

We proposed a methodology that allows the mapping of the maximum potential run-out, the velocity and dynamic pressure of PDCs that are smaller than $10^7 m^3$. More data on larger volumes, mobility and velocity could be considered to improve this approach and reduce the uncertainty of its predictions.

Run-outs and velocities can be predicted within reasonable levels of uncertainty and while hazard maps should be of at least 0.8 km horizontal scale, velocities can be predicted within 3 m s^{-1}. Additional safety margins can be incorporated into hazard maps by using the confidence limits of the regression models implemented. This kind of information is crucial and is rarely considered in hazard assessment. Sensitivity analysis to evaluate the effects of different sources of uncertainty (e.g. errors in the input volumes) would contribute towards the improvement of the methodology in these respects.

We were able to observe an important level of consistency between the output runs of the approach proposed and data on pyroclastic flow events that occurred at Unzen and Mayon volcanoes. This is promising, as regards the application of the proposed methodology for hazard mapping in other volcanoes. For application and testing by other users, the software template is available upon request to the corresponding author. We expect to make it public and downloadable in ESRI's website for codes/scripts in the near future.

Acknowledgements This research was possible thanks to the funding provided by the European Union through the project Explosive Eruption Risk and Decision Support for EU Populations Threatened by Volcanoes (EXPLORIS) EVR1-2001-00047. We thank two anonymous reviewers for constructive comments that improved the paper.

References

Alberico I, Lirer L, Petrosino P, Scandone R (2002) A methodology for the evaluation of long-term volcanic risk from pyroclastic flows in Campi Flegrei (Italy). J Volcanol Geotherm Res 116: 63–78

Alvarado GE, Soto GJ (2002) Pyroclastic flow generated by crater-wall collapse and outpouring of the lava pool of Arenal Volcano, Costa Rica. Bull Volcanol 63:557–568

Burrough PA, McDonnel RA (1999) Principles of Geographical Information Systems. Oxford University Press, Oxford, New York, pp 333

Calder ES, Cole PD, Dade WB, Druitt TH, Hoblitt RP, Huppert HE, Ritchie L, Sparks RSJ, Young SR (1999) Mobility of pyroclastic flows and surges at the Soufrière Hills Volcano, Montserrat. Geophysical Res Lett 26(5):540–637

Calder ES, Luckett R, Sparks RSJ, Voight B (2002) Mechanisms of lava dome instability and generation of rockfalls and pyroclastic flows at Soufrière Hills Volcano, Montserrat. In: Druitt

TH, Kokelaar BP (eds), The Eruption of Soufrière Hills Volcano, Montserrat, from 1995 to 1999. Geological Society of London Memoirs 21, 173–190
Cole PD, Calder ES, Sparks RSJ, Clarke AB, Druitt TH, Young SR, Herd RA, Harford CL, Norton GE (2002) Deposits from dome-collapse and fountain-collapse pyroclastic flows at Soufrière Hills Volcano, Montserrat. In: Druitt TH, Kokelaar BP (eds), The Eruption of Soufrière Hills Volcano, Montserrat, from 1995 to 1999. Geological Society of London Memoirs 21, 231–262
Cole PD, Fernandez E, Duarte E, Duncan AM (2005) Explosive activity and pyroclastic flow formation at Arenal volcano, Costa Rica 1987–2001. Bull Volcanol (in press)
Draper NR, Smith H (1966). Applied regression analysis. Wiley, New York
Esposti Ongaro T, Neri A, Todesco M, Macedonio G (2002) Pyroclastic flow hazard assessment at Vesuvius (Italy) by using numerical modelling. II. Analysis of flow variables. Bull Volcanol 64:178–191
Hayashi JN, Self S (1992) A comparison of pyroclastic flow and debris avalanche mobility. J Geophysical Res 97(B6):9063–9071
Hoblitt RP (1986) Observations of the eruptions of July 22 and August 7 1980 at Mt. St. Helens. Washington, USGS Professional Paper 1335
Hsü J (1975) Catastrophic debris streams (sturzstroms) generated by rockfalls. Geologic Soc Am Bull 86:129–140
Iverson RM (1997) The physics of debris flows. Rev Geophys 35:245–296
Loughlin SC, Calder ES, Clarke A, Cole PD, Luckett R, Mangan MT, Pyle DM, Sparks RSJ, Voight B, Watts RB (2002) Pyroclastic flows and surges generated by the 25 June 1997 dome collapse, Soufrière Hills Volcano, Montserrat. In: Druitt TH, Kokelaar BP (eds), The Eruption of Soufrière Hills Volcano, Montserrat, from 1995 to 1999. Geological Society, London Memoirs, 21:191–209
Levine AH, Kiefer SW (1991) Hydraulics of the August 7 1980 pyroclastic flow at Mount St. Helens, Washington. Geology 19(11):1121–1124
Malin MC, Sheridan MF (1982) Computer-Assisted mapping of pyroclastic surges. Science 217:637–640
McEwen M, Malin MC (1989) Dynamics of Mt. St. Helens' 1980 pyroclastic flows, rockslide-avalanche, lahars and blast. J Volcanol Geotherm Res 37:205–231
Moore JG, Melson WG (1969) Nuées Ardentes of the 1968 Eruption of Mayon Volcano, Philippines. Bull Volcanol 33:600–620
Nakada S, Shimizu H, Ohta K (1999) Overview of the 1990–1995 eruption at Unzen volcano. J Volcanol Geoth Res 89:1–22
Renschler CS (2005) Scales and Uncertainties in volcano hazard prediction – optimizing the use of GIS and models. J Volcanol Geoth Res 139(1–2):73–87
Saucedo R, Macías JL, Sheridan MF, Bursik MI, Komorowski JC (2005) Modelling of pyroclastic flows of Colima Volcano, Mexico: Application to hazard assessment. J Volcanol Geotherm Res 139:103–115
Sheridan M, Macías JL (1992) PC Software for 2-Dimensional gravity-driven flows: Applications to the Colima and El Chichón volcanoes, Mexico. In: Proc. 2nd Reunion Int. Volcanol., Colima, Mexico, 5
Sheridan M, Malin M (1983) Application of computer-assisted mapping to volcanic hazard evaluation of surge eruptions: Vulcano, Lipari. J Volcanol Geotherm Res 17:187–202
Sheridan MF, Hubbard B, Carrasco-Nuñez G, Siebe C (2004) Pyroclastic Flow Hazard at Volcán Citlaltépetl. Natural Hazards 33:209–221
Sheridan MF, Hubbard B, Carrasco-Nuñez G, Siebe C (2000) GIS model for volcanic hazard assessment: pyroclastic flows at Volcán Citlaltépetl, México. In: Parks BO, Clarke KM, Crane MP (eds), Proc. 4th international conference on integrating geographic information systems and environmental modeling: problems, prospects, and needs for research, Boulder, University of Colorado, USA
Siebert L (1984) Large volcanic debris avalanches: Characteristics of source areas, deposits and associated eruptions. J Volcanol Geotherm Res 22:163–197
Spence RJS, Baxter PJ, Zuccaro G (2004) Building vulnerability and human casualty estimation for a pyroclastic flow: a model and its application to Vesuvius. J Volcanol Geotherm Res 133:321–343
Todesco M, Neri A, Esposti Ongaro T, Papale P, Macedonio G, Santacroce R, Longo A (2002) Pyroclastic flow hazard assessment at Vesuvius (Italy) by using numerical modelling. I. Large-scale dynamics. Bull Volcanol 64:155–177
Valentine GA (1998) Damage to structures by pyroclastic flows and surges, inferred from nuclear weapons effects. J Volcanol Geotherm Res 87:117–140